



Influence of linear-axis error motions on simultaneous three-axis controlled motion accuracy defined in ISO 10791-6

Kenno, Takaaki
Sato, Ryuta
Shirase, Keiichi
Natsume, Shigemasa
Spaan, Henny A. M.

(Citation)

Precision Engineering, 61:110-119

(Issue Date)

2020-01

(Resource Type)

journal article

(Version)

Accepted Manuscript

(Rights)

© 2019 Elsevier.

This manuscript version is made available under the CC-BY-NC-ND 4.0 license
<http://creativecommons.org/licenses/by-nc-nd/4.0/>

(URL)

<https://hdl.handle.net/20.500.14094/90006676>



Influence of linear-axis error motions on simultaneous three-axis controlled motion accuracy defined in ISO 10791-6

Takaaki Kenno ¹⁾, Ryuta Sato ¹⁾, Keiichi Shirase ¹⁾
Shigemasa Natsume ²⁾, Henny A.M. Spaan ³⁾

1) Department of Mechanical Engineering, Kobe University
1-1 Rokko-dai, Nada, Kobe 657-8501, JAPAN
TEL/FAX: +81-78-803-6326
Email: sato@mech.kobe-u.ac.jp

2) P & C LTD.

3) IBS Precision Engineering BV

Abstract

Five-axis machine tools, which combine three linear axes and two rotary axes, are required for accuracy in machining complex shapes. In this paper, to clarify the influence of simultaneous three-axis control motion measurements as specified in ISO 10791-6, the measured results using a ball bar and R-test are compared. As the motion trajectories of the linear axes are not identical in both measurement devices, it is expected that the error motions of the linear axes cause different measurement results depending on the measurement devices. Thus, the squareness errors between the linear axes and the error motions of the linear axes are assumed as error factors that influence the measured results in this study. A mathematical model of a five-axis control machine tool that considers the error motions and squareness errors of the linear axis is constructed, and the influence of those error factors on motion accuracy is examined using an experiment and a simulation. As a result, the squareness errors and error motions of the linear axis are observed to greatly affect simultaneous three-axis controlled motion accuracy.

Keywords

Five-axis controlled machine tools, Simultaneous three-axis motion, Error motion, Ball bar, R-test

1 Introduction

Five-axis controlled machine tools that have three linear axes and two rotary axes can control both the relative position and relative angle between the tool and the workpiece. These machine tools can machine complex shapes such as impellers. In addition, five-axis controlled machine tools enable machining without requiring setup replacement, even in machining that requires the setup replacement of a workpiece with conventional three-axis control machine tools. Although many advantages exist, five-axis controlled machine tools have inferior machining accuracy compared to three-axis controlled machine tools because the former have more error sources such as geometrical errors between the axes owing to the addition of rotary axes according to the ISO 230-1 and ISO 230-7 standards [1, 2]. Hence, it is required to evaluate the errors appropriately.

Till date, an accuracy evaluation method for five-axis controlled machine tools has not been defined, but motion accuracy evaluation methods corresponding to five-axis controlled machine tools were in effect as of the ISO 10791-6 standard [3] in 2014. The standard defines simultaneous three-axis movements with two linear axes and a rotary axis to evaluate the accuracy of interpolation in five-axis machining centers. Furthermore, the ball bar and R-test [flat-ended linear displacement sensor(s) or a sensor's nest] are specified as the measuring devices.

The ball bar is a device that can measure the relative motion error between two balls installed on the spindle and the table, and is widely used as a measuring device for circular motion accuracy tests [4, 5]. By contrast, the R-test, which is a measuring device for flat-ended linear displacement sensors, was developed in recent years and measures the relative displacement between the spindle and the table as well as the ball bar. The R-test is useful because it can measure the X, Y, and Z directions simultaneously without contact [6].

In recent years, many research studies based on ISO 10791-6 [3] have been conducted. Zhong et al. [7] performed simultaneous three-axis controlled motion measurements according to ISO 10791-6 [3] using a ball bar and evaluated the motion accuracy of a five-axis controlled machine tool. Yamaji et al. [8] applied an R-test to evaluate the motion accuracy according to ISO 10791-6 [3]. Furthermore, with regard to the relationship between the machining and motion accuracies, Florussen et al. [9] simultaneously performed measurement experiments and processing experiments using R-tests, and it was revealed that the motion accuracy has a large effect on the machining accuracy. Inasaki et al. [10] and Tsutsumi et al. [11] succeeded in improving the accuracy by performing simultaneous three-axis controlled motion measurements and identifying the geometric errors determined by the kinematic model of a machine tool.

However, although motion accuracy evaluations using a ball bar and R-test have been conducted by many researchers [12, 13, 14], the differences in the measurement results of the two measurement devices have not been compared in detail. Identifying the error factors that influence the measured results of each device to appropriately evaluate the accuracy of five-axis controlled machine tools is important. The purpose of this

research is to clarify the factors affecting the measured results and the differences in the results when using the ball bar and R-test. As the motion trajectory of the linear axes is not identical for both measurement devices, it is expected that the error motions of the linear axes [1] cause the different measurement results depending on the measurement devices.

To achieve the purpose of this study, simultaneous three-axis controlled motions specified in ISO 10791-6 [3] are conducted and measured by a ball bar and R-test for comparison. The squareness errors between the linear axes and the error motions of the linear axes are assumed as error factors that affect the measurements in this study. In order to verify the influence of those error factors on motion accuracy, simulations of motions with squareness errors and error motions are carried out [15]. The error motions of the linear axes are evaluated by using a laser interferometer.

This paper is organized as follows. First, in Chapter 2, measurement method for simultaneous three-axis controlled motions by the ball bar and R-test are introduced. Chapter 3 introduces the measurement method for the error motions of the linear axes and squareness errors between the linear axes. A kinematics model considering the errors is used. In Chapter 4, the factors that influence the measurement results are investigated by comparing the measurement results and simulation results of simultaneous three-axis controlled motions in a ball bar and R-test. Finally, the conclusions are summarized in Chapter 5.

2 Accuracy evaluation method for five-axis controlled machine tool

2.1 Structural configuration of five-axis controlled machine tool

The structural configuration of five-axis controlled machine tools is classified into three types in the ISO 10791-6 standard [3]: machines with two rotary axes in the spindle head (A-type), machines with two rotary axes on the workpiece side (B-type), and machines with a swivel head and/or a rotary table (C-type). The accuracy evaluation methods are described for each configuration type. The vertical-type five-axis controlled machining center “NMV1500 DCG HSC” used in this study is classified as a machine with two rotary axes on the workpiece side (B-type). Three linear axes (X, Y, and Z axes) are located on the spindle side, and two rotary axes (B and C axes) are located on the worktable side in the machining center. This machine has a structure in which the X-axis is on the Y-axis and the Z-axis is on the X-axis. ISO 10791-6 [3] shows four types of movements (BK1 to BK4) as methods for evaluating the accuracy of a five-axis controlled machine tool with two rotary axes on the workpiece side. BK1 and BK2 are evaluation methods based on simultaneous three-axis controlled motions with two linear axes and a rotary axis, and BK3 and BK4 are evaluation methods with simultaneous five-axis controlled motions. The influence of error factors on the accuracy of simultaneous three-axes controlled motions BK1 and BK2 are investigated in this study.

2.2 Ball bar and R-test

In the ISO 10791-6 standard [3], the ball bar and R-test (flat-ended linear displacement sensors or a sensor's nest) are specified as measuring devices. The ball bar has steel balls installed on the spindle side and the workpiece side, and can measure the relative displacement between the steel balls. The ball bar is widely used for circular motion tests of conventional three-axis controlled machine tools. The R-test is a device recently developed for five-axis control machine tools. Similar to the ball bar in that it measures the relative displacement between the spindle and the table, the displacement in the X, Y, and Z directions can also be measured simultaneously by one reference sphere and three displacement sensors.

Although it is assumed that the measurement results by the two measurement devices are identical, there is no example to verify the difference in the results when compared with the details. Therefore, it is necessary to verify the influence of different measurement methods and to clarify the cause if the measurement results are different. In this study, a ball bar system (QC20W, Renishaw plc.) as shown in **Figure 1** (a) and an R-test system (Trinity, IBS Precision Engineering bv.) as shown in **Figure 1** (b) are applied for the measurements. The next section shows the measurement methods using each measurement device for simultaneous three-axis controlled motions.

2.3 Simultaneous three-axis controlled motions

The motion accuracy evaluation methods specified in BK2 of ISO 10791-6 [3] are shown in **Figure 2**. BK2 performs simultaneous three-axis controlled motion. This creates a circular interpolation motion by the X-axis and Y-axis in the XY-plane simultaneously with the rotation of the C-axis. BK2 can evaluate the synchronous motion accuracy between the X-, Y-, and C-axes. In this study, measurements are performed for the ball bar and R-test. In case of the ball bar, measurements are performed by changing the sensitivity direction of the ball bar to the radial direction, axial direction, and tangential direction with respect to the C-axis rotational center. By contrast, the R-test can measure the displacement in three directions simultaneously; hence, the measurements that were required three times with the ball bar can be measured at the same time.

Regarding the measurement method for the ball bar measurement, the sensitivity direction of the ball bar is directed in the radial direction, axial direction, and tangential direction of the C-axis rotational center as shown in **Figures 2** (a), (b), and (c), respectively. For measurement in the radial and tangential directions, since the movable range of the machine tool is limited, the reference length of the ball bar was changed from 100 mm to 50 mm by using a small circle kit. In addition, according to ISO 10791-6, the feed rate of the rotary axis is set to 360°/min in each measurement. In order to avoid the influence of the start and end of the motions, the motion was performed at 720° and 180° before and after the end and start of the measurement were removed, respectively. In addition, measurements in both the clockwise and counterclockwise directions were performed, taking into consideration the influence of different motion directions.

In the measurement by the R-test, the setting position of the reference ball on the workpiece side was the same as in the measurement by the ball bar. The measurement was performed, as shown in **Figure 2(d)**. The feed rate for the measurement was also set to 360°/min.

The motion accuracy evaluation method specified in BK1 of ISO10791-6 [3] is shown in **Figure 3**. This creates a circular interpolation motion by the Z-axis and X-axis in the ZX-plane simultaneously with the rotation of the B-axis. As in the case of BK2 mentioned above, in the case of the ball bar, the sensitivity direction is changed in three ways. By contrast, in case of the R-test, the error in three directions is evaluated in one movement.

Regarding the method for ball bar measurement, **Figures 3(a)** and **(b)** show the measurement methods with the sensitivity direction of the ball bar directed in the radial and axial directions of the B-axis rotational center. Unfortunately, it was impossible to direct the sensitivity direction of the ball bar toward the tangential direction of the B-axis rotational center because the tool holder and ball bar interfered with each other. Although it was possible to perform B-axis rotation of only 90° in the measurement of the B-axis tangential direction, it is difficult to evaluate the eccentricity of the circular arc from the measurement results, and comparison with other results is difficult. Therefore, in this study, the measurement of the B-axis in the tangential direction by the ball bar was not performed. The measurement method by R-test is shown in **Figure 3(c)**. In this case, the measurement in the tangential direction, which is difficult to evaluate by ball bar measurement, can be evaluated by the B-axis rotation of 180°.

3. Error motions and squareness errors of linear axes

3.1 Error motions of linear axes

3.1.1 Error motion measurement by laser interferometer

In this study, the error motions of the linear X-, Y-, and Z-axes are evaluated by using a laser interferometer system (XL-80, Renishaw plc.). This system can measure angular error motions in the pitch and yaw directions, the linear positioning error motion, and the two straightness error motions of the linear axes. One of the angular error motions (roll) cannot be measured by the system. Hence, the error motions in five directions excluding the roll direction are evaluated and modeled in this study. Measurements of each error motion are performed at points with 20-mm intervals in the measurable range in each of the X-, Y-, and Z-axes. In addition, the deviations are evaluated as the average values of five-time measurements in both motion directions to reduce the influence of the motion direction and the repeatability.

Figure 4 shows the measurement setups to measure the Y- and X-axis positioning error motions as examples. **Figure 5** shows the measured error motions in five directions of the X-axis. According to the **Figure 5 (a)**, the positioning deviation becomes larger depending on the displacement. This results from the pitch error of the ball screw because the axis has a semiclosed-loop control system. It can also be seen that the straightness

error along the Y-axis (E_{YX}) is larger than the error along the Z-axis (E_{ZX}). The angular error motion around the Y-axis (E_{BX}) is also larger than the error around the Z-axis (E_{CX}).

3.1.2 Conversion of positioning and straightness deviations to reference position

Although angular error motions of the X-axis are the same regardless of the position of both the Y-axis and Z-axis, the X-axis measurements of both linear positioning error motion and two straightness error motions are influenced by the position of both Y-axis and Z-axis. This is because it is affected by angular error motions of the X-axis (It is detailed in [1]). If the measured Y and Z coordinates and angular error motions of the X-axis are known, the measured values of both linear positioning and straightness error motions of the X-axis can be converted in any Y and Z coordinates. Similarly, the conversion can be performed on the measured values of Y- and Z-axis the error motions.

In this study, the reference position for all error motions are defined at the zero positions of the axes in the model for simulations. Therefore, the measured values of the deviations of X-, Y-, and Z-axis should be converted to the deviations on the straight lines that passing through the reference position. The conversion method can be described as follows using the linear positioning error motion of the X-axis as an example.

Based on the reference position ($x_{ref}, y_{ref}, z_{ref}$), the Y- and Z-axis position when the measurement of X-axis error (y_{EXX}, z_{EXX}), and the measured values of deviations $E_{XX}(x)$, $E_{YX}(x)$, and $E_{ZX}(x)$, the X-axis deviations at the reference position of Y- and Z-axis ($E'_{XX}(x)$, $E'_{YX}(x)$, and $E'_{ZX}(x)$) can be calculated as shown in Equation (1). The reference position is set to ($x_{ref}, y_{ref}, z_{ref}$) = (-140, 100, 320) in this study. On the other hand, the measurement of X-axis error motions are performed at (y_{EXX}, z_{EXX}) = (100, 135). The differences between the reference and measurement positions of Y- and Z-axis influences the measured values of the deviations of X-axis owing to the angular error motions of the axes. **Figure 6** shows the measured and converted positioning deviations of X-axis as an example. The differences mainly owing to the angular error motion of X-axis, E_{BX} . The other error motions of the axes can also be converted by the Equations (2) and (3)

$$\left. \begin{aligned} E_{XX}'(x) &= E_{XX}(x) - E_{BX}(x) \cdot (z_{EXX} - z_{ref}) + E_{CX}(x) \cdot (y_{EXX} - y_{ref}) \\ E_{YX}'(x) &= E_{YX}(x) + E_{AX}(x) \cdot (z_{EYX} - z_{ref}) - E_{CX}(x) \cdot (x_{EYX} - x_{ref}) \\ E_{ZX}'(x) &= E_{ZX}(x) - E_{AX}(x) \cdot (y_{EZX} - y_{ref}) + E_{BX}(x) \cdot (x_{EZX} - x_{ref}) \end{aligned} \right\} \quad (1)$$

$$\left. \begin{aligned} E_{XY}'(y) &= E_{XY}(y) - E_{BY}(y) \cdot (z_{EXY} - z_{ref}) + E_{CY}(y) \cdot (y_{EXY} - y_{ref}) \\ E_{YY}'(y) &= E_{YY}(y) + E_{AY}(y) \cdot (z_{EYY} - z_{ref}) - E_{CY}(y) \cdot (x_{EYY} - x_{ref}) \\ E_{ZY}'(y) &= E_{ZY}(y) - E_{AY}(y) \cdot (y_{EZY} - y_{ref}) + E_{BY}(y) \cdot (x_{EZY} - x_{ref}) \end{aligned} \right\} \quad (2)$$

$$\left. \begin{aligned} E_{XZ}'(z) &= E_{XZ}(z) - E_{BZ}(z) \cdot (z_{EXZ} - z_{ref}) + E_{CZ}(z) \cdot (y_{EXZ} - y_{ref}) \\ E_{YZ}'(z) &= E_{YZ}(z) + E_{AZ}(z) \cdot (z_{EYZ} - z_{ref}) - E_{CZ}(z) \cdot (x_{EYZ} - x_{ref}) \\ E_{ZZ}'(z) &= E_{ZZ}(z) - E_{AZ}(z) \cdot (y_{EZZ} - y_{ref}) + E_{BZ}(z) \cdot (x_{EZZ} - x_{ref}) \end{aligned} \right\} \quad (3)$$

3.2 Squareness errors between the linear axes

3.2.1 Influence of squareness errors

The squareness errors between the linear axes causes the contouring error. As all three linear axes are arranged onto the spindle side in the five-axis controlled machine tools used herein, the squareness errors affect the position of the tool center point. The circular arc trajectory in the circular test is deformed into an elliptical shape owing to the squareness errors [5]. The circular test is a method to evaluate the motion accuracy of the linear axes by two linear-axis synchronous motions.

Figure 7 shows the effect of squareness errors between the linear axes on the circular trajectories of the circular motions in the XY, YZ, and ZX planes. The positional errors (Δy and Δz) can be expressed as Equation (4). The squareness errors can be defined as γ_{XY} , α_{XZ} , and β_{XZ} .

$$\left. \begin{aligned} \Delta y &= \gamma_{XY}X \\ \Delta z &= \alpha_{XZ}Y \\ \Delta z &= -\beta_{XZ}X \end{aligned} \right\} \quad (4)$$

3.2.2 Circular motion tests to identify squareness errors

Three squareness errors between the axes are identified by the measured circular trajectories. The circular motion test is performed in three planes XY, YZ, and ZX, as shown in **Figure 8**. During XY plane measurement, circular motion is performed twice. Then measuring range is setup 360° excluding 180° before and after measuring range. However, during YZ and ZX plane measurement, circular motions are performed only 180° owing to the interference problem. The feed rate is set to $360^\circ/\text{min}$, and the measurements are performed for both the clockwise and counterclockwise directions, taking into consideration the influence of different motion directions. The measured circular trajectories shown herein are the averaged trajectories of the measured results in both the motion directions.

The squareness errors are identified by applying the regression approach between the measured and simulated circular trajectories.

Table. 1 Identified squareness errors based on circular trajectories

γ_{xy}	-0.0014°
β_{xz}	-0.0020°
α_{xz}	-0.00039°

Figure 9 shows the measured and simulated circular trajectories with the identified squareness errors listed in **Table 1**. It can be seen from the figure and table that the

squareness errors between the X- and Y-axis or X- and Z-axis are larger than the error between the Y- and Z-axis.

3.3 Simulation with error motions and squareness errors

The effect of the error motions of the linear axes and the squareness errors on the relative motion between the tool and the table can be expressed using a homogeneous transformation matrix considering the errors. The five-axis control machining center used herein has a structure wherein the X-axis is on the Y-axis and the Z-axis is on the X-axis. By performing coordinate transformation based on the order from the Z-axis coordinate system to the X-axis coordinate system, the Y-axis coordinate system, and the machine coordinate system, expressing the influence of the error motions of the linear axis is possible, as shown in Equations (5) and (6). Here, e_x , e_y , e_z , e_a , e_b , and e_c , as shown in Equation (7), denote the three position errors and three angular errors of the tool center point considering the error motions. Equation (7) also contains the squareness errors.

$$\begin{bmatrix} {}^m p \\ 1 \end{bmatrix} = {}^m T_y {}^y T_x {}^x T_z \begin{bmatrix} 0 \\ 0 \\ 0 \\ 1 \end{bmatrix} \approx \begin{bmatrix} 1 & -e_c & e_b & x + e_x \\ e_c & 1 & e_a & y + e_y \\ -e_b & e_a & 1 & z + e_z \\ 0 & 0 & 0 & 1 \end{bmatrix} \quad (5)$$

$$\left. \begin{aligned} {}^x T_z &= D_z(z) \cdot D_x(E_{XZ}(z)) \cdot D_y(E_{YZ}(z)) \cdot D_z(E_{ZZ}(z)) \cdot D_a(E_{AZ}(z)) \cdot D_b(E_{BZ}(z)) \cdot D_c(E_{CZ}(z)) \\ {}^y T_x &= D_x(x) \cdot D_x(E_{XX}(x)) \cdot D_y(E_{YX}(x)) \cdot D_z(E_{ZX}(x)) \cdot D_a(E_{AX}(x)) \cdot D_b(E_{BX}(x)) \cdot D_c(E_{CX}(x)) \\ {}^m T_y &= D_y(y) \cdot D_x(E_{XY}(y)) \cdot D_y(E_{YY}(y)) \cdot D_z(E_{ZY}(y)) \cdot D_a(E_{AY}(y)) \cdot D_b(E_{BY}(y)) \cdot D_c(E_{CY}(y)) \end{aligned} \right\} \quad (6)$$

$$\left. \begin{aligned} e_x(x,y,z) &= E_{XX}(x) + E_{XY}(y) + E_{XZ}(z) + ((E_{BX}(x) + (E_{BY}(y)))z \\ e_y(x,y,z) &= E_{YX}(x) + E_{YY}(y) + E_{YZ}(z) - (E_{AY}(y) + E_{AX}(x))z + (E_{CY}(y))x - \gamma_{xy}x \\ e_z(x,y,z) &= E_{ZX}(x) + E_{ZY}(y) + E_{ZZ}(z) - E_{BY}(y)x + \beta_{xz}x + \alpha_{xz}y \\ e_a(x,y,z) &= E_{AX}(x) + E_{AY}(y) + E_{AZ}(z) \\ e_b(x,y,z) &= E_{BX}(x) + E_{BY}(y) + E_{BZ}(z) \\ e_c(x,y,z) &= E_{CX}(x) + E_{CY}(y) + E_{CZ}(z) \end{aligned} \right\} \quad (7)$$

Figure 10 shows the estimated volumetric error of the tool center point with the influence of the error motions and squareness errors of the linear axis. The positional errors at each point are magnified 10,000 times. The circles in the figure indicate the circular trajectories with and without the error motions of the linear axes.

Figure 11 shows the measured and simulated circular trajectories with both the error motions and squareness errors. In particular, the simulated trajectory on the XY plane shown in the **Figure 11** (a) matches the measured trajectory more accurately than the simulation results shown in **Figure 9** (a). It is clear from the results that the error motions of the linear axes influence the circular trajectories. The validity a mathematical model considering the error motions of the linear axis and the squareness errors between the linear axes can be confirmed by comparing measured results and simulation results of

circular tests.

However, the trajectory on the ZX plane does not accurately match the measured one. Although it is expected that the roll errors that cannot be measured in this study affect the results, the reason cannot be clarified at this time.

4. Simultaneous three-axis control motion

4.1 Comparison of measured results by ball bar and R-test

The simultaneous three-axis control motions measured by the ball bar and R-test are compared in this study. Measurements and simulations are performed according to the methods described in the previous chapters. **Figures 12** and **13** show the measured and simulated results of the measurement results by a ball bar and R-test. According to the figures, in comparing the results of the ball bar and R-test, a difference can be observed between the results, especially in the radial direction measurements [**Figure 12** (a) and (b) and **Figure 13** (a) and (b)]. Regarding the measurements in the radial direction, the motion trajectory of the linear axes is not identical for both measurement methods, as shown in **Figure 14**. It can be expected that the effects of the error motions and squareness errors of the linear axes are different in the measurements using a ball bar and R-test.

4.2 Comparison of measurements by identical motion trajectory of linear axes

The difference between the measured results of the ball bar and R-test are expected to be caused by the difference between the motion trajectories of the linear axis. Hence, the motion trajectory of the linear axes for the measurements the by ball bar is designed to be the same as that for the R-test, as shown in **Figure 15**.

The measured and simulated results of the simultaneous three-axis motions are shown in **Figures 16** and **17**. The error motions of the linear axes and the squareness errors between the linear axes are taken into the model in the simulation. In comparing **Figures 16** (a) and **12** (a), and **Figure 17** (a) and **13** (a), the measured and simulated results differed from each other. The measured and simulated results with identical motion trajectories of the linear axes using the R-test shown in **Figures 16** and **17** are identical to the measured and simulated results of the R-test shown in **Figure 12** (b), (d), and **Figure 13** (b), (d).

As described above, it is confirmed that the error motions of the linear axes and the squareness errors significantly affect the measured results of the simultaneous three-axis controlled motions. This fact was confirmed by both the actual measurements and the simulations. The results of this study suggest that the evaluated results using the simultaneous three-axis motions defined in ISO 10791-6 are affected by the error motions and squareness errors of the linear axes, and that the influence of the errors depends on the measurement setup of the tests. Furthermore, it has confirmed from both of the measured and simulated results that the measured results using a ball bar coincided with the results using an R-test by designing the motion trajectory of the linear axes identically for the two measurement methods.

5. Conclusion

In this study, in order to clarify the factors that affect the motion accuracy evaluation results of five-axis control machine tools based on ISO 10791-6, the measurement and identification of the error motions and squareness errors of linear axes were conducted. The factors affecting the measured results and the differences in the results were evaluated by using a ball bar and R-test. Furthermore, a mathematical model of a five-axis control machine tool that considered the error motions of the linear axis and the squareness errors of the linear axis was constructed. The influence of those error factors on motion accuracy was examined from both an experiment and simulation. The conclusions can be summarized as follows:

- (1) A mathematical model considering the error motions of the linear axis and the squareness errors between the linear axes was developed, and the validity of the model was confirmed by comparing measured results and simulation results of circular tests.
- (2) The measured results in the radial, axial, and tangential directions in simultaneous three-axis controlled motion measurements by the ball bar and R-test can be expressed by simulations using the mathematical model by using the error motions and squareness errors of the linear axes.
- (3) It was confirmed that the measured results differed significantly owing to the difference in the motion trajectory of the linear axis in the simultaneous three-axis control motion. Furthermore, by designing the motion trajectory of the linear axes identically for the two measurement methods, the measured results using a ball bar coincided with the results using an R-test.

Accurately evaluating the motion accuracy first to improve the accuracy of five-axis control machine tools is essential. The results of this study suggest that the evaluated results by the simultaneous three-axis motions defined in ISO 10791-6 are affected by the error motions and squareness errors of the linear axes, and the influence of the errors depends on the measurement setup of the tests. In a future study, we will try to evaluate the influence of error motions of the rotary axes on the motion accuracy evaluation results of five-axis control machine tools.

Acknowledgements

This study was financially supported by the Machine Tool Engineering Foundation. The authors would also like to acknowledge the extensive support of the Machine Tool Technologies Research Foundation and DMG MORI Co., Ltd.

Reference

- [1] ISO 230-1, Test Code for Machine Tools, Part 1: Geometric Accuracy of Machines Operating under No-Load or Quasi-Static Conditions, 2012.
- [2] ISO 230-7, The Code for Machine Tools, Part 7: Geometric Accuracy of Axes of Rotation, 2015.
- [3] ISO 10791-6, Test Conditions for Machining Centers, Part 6: Accuracy of Speeds and Interpolations, 2014.
- [4] Kuric, I., Kosinar, M., Cisar, M., Measurement and analysis of CNC machine tool accuracy in different location on work table, *Proceedings in Manufacturing systems*, Vol. 7, 2012; 259–264.
- [5] ISO 230-4, Test Code for Machine Tools, Part 4: Circular Tests for Numerically Controlled Machine Tools, 2005.
- [6] Weikert, S., R-test: A new device for accuracy measurements on five axis machine tools, *CIRP Ann-Manuf Technol*, Vol. 53, 2004; 429–432.
- [7] Zhong, L., Bi, Q., Wang, Y., Volumetric accuracy evaluation for five-axis machine tools by modeling spherical deviation based on double ball-bar kinematic test, *International Journal of Machine Tools and Manufacture*, Vol. 122, 2017; 106–119.
- [8] Yamaji, M., Hamabata, N., Ihara, Y., Evaluation of linear axis motion error of machine tools using an R-test device, *Procedia CIRP*, Vol. 14, 2014; 311–316.
- [9] Florussen, G.H.J., Spaan, H.A.M., Spaan-Burke, T.M., Verifying the accuracy of five-axis machine tool focused on kinematic ISO tests using a torus-shaped test work piece, *Procedia Manufacturing*, Vol. 14, 2017; 58–65.
- [10] Inasaki, I., Kishinami, K., Sakamoto, S., Sugimura, N., Takeuchi, Y., Tanaka, F., *Form shaping theory of machine tools: Fundamentals and applications*, Yokendo, Tokyo; 1997 (in Japanese).
- [11] Tsutsumi, M., Tone, S., Kato, N., Sato, R., Enhancement of geometric accuracy of five-axis machining centers based on identification and compensation of geometric deviations, *International Journal of Machine Tools & Manufacture*, Vol. 68, 2013; 11–20.
- [12] Ibaraki, S., Tsujimoto, S., Nagai, Y., Sakai, Y., Morimoto, S., Miyazaki, Y., A pyramid-shaped machining test to identify rotary axis error motions on five-axis error motions on five-axis machine tools: Software development and a case study, *Int J Adv Manuf Technol*, Vol. 94, 2018; 227–237.
- [13] Bringmann, B., Knapp, W., Machine tool calibration: Geometric test uncertainty depends on machine tool performance, *Precision Engineering*, Vol. 33, 2009; 524–529.
- [14] Hong, C., Ibaraki, S., Matsubara, A., Influence of position-dependent geometric errors of rotary axes on a machining test cone frustum by five-axis machine tools, *Precision Engineering*, Vol. 35, 2011; 1–11.
- [15] Ibaraki, S., Knapp, W., Indirect measurement of volumetric accuracy for three-axis and five-axis machine tools: A review, *Int. J. of Automation Technology*, Vol. 6, 2012; 110–124.

Figures:

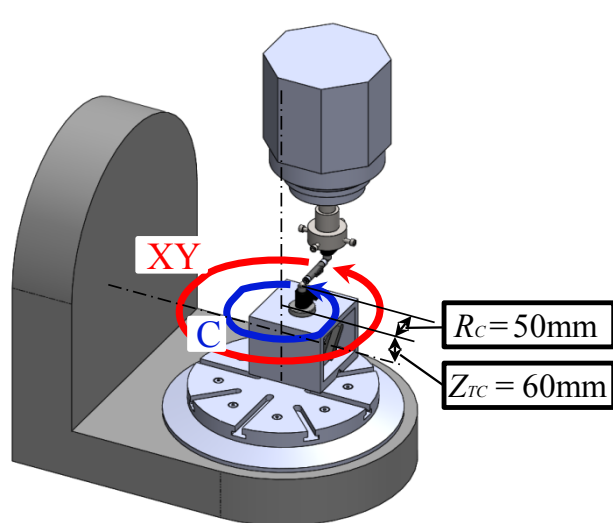


(a) Ball bar

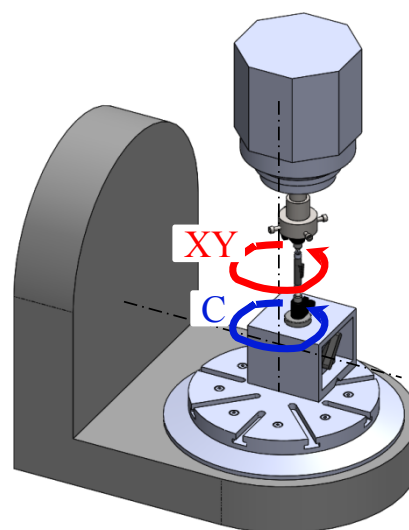


(b) R-test

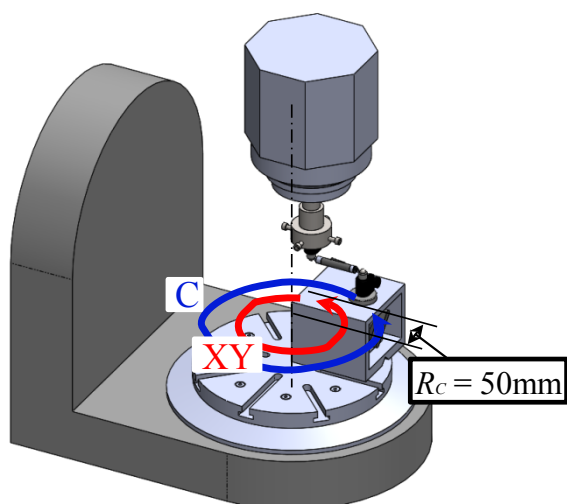
Figure 1 Measuring devices specified in ISO 10791-6



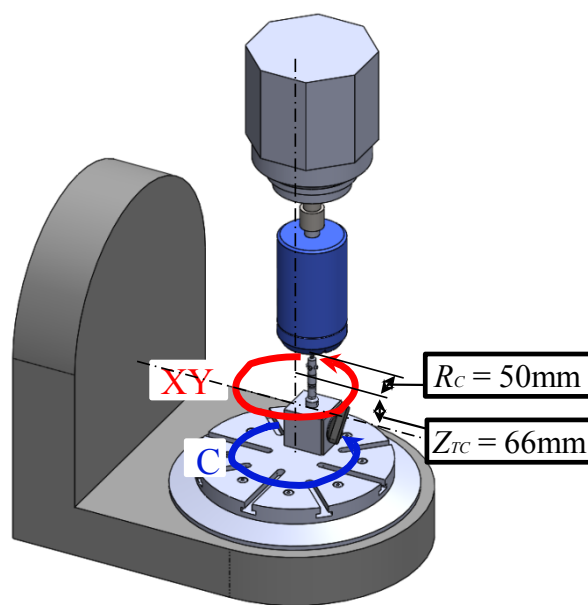
(a) C-axis radial direction



(b) C-axis axial direction

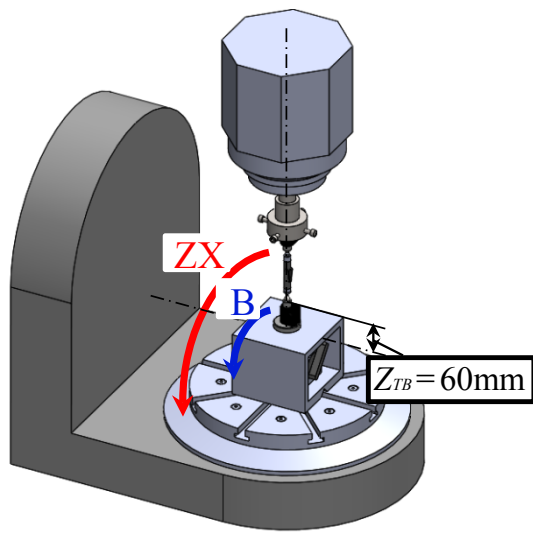


(c) C-axis tangential direction

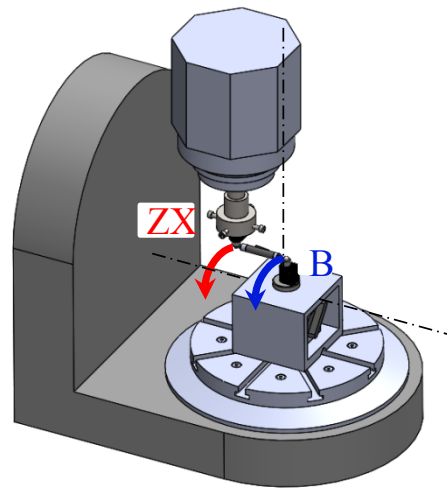


(d) Measurement by R-test

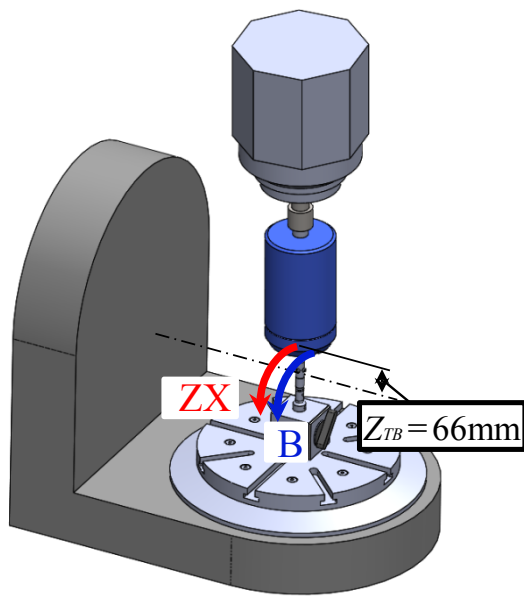
Figure 2 Simultaneous three-axis controlled motion (X-, Y-, and C-axes)



(a) B-axis radial direction



(b) B-axis axial direction



(c) Measurement by R-test

Figure 3 Simultaneous three-axis controlled motion (Z-, X-, and B-axes)

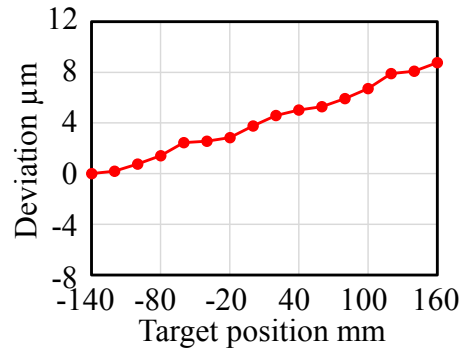


(a) Positioning error of Y-axis

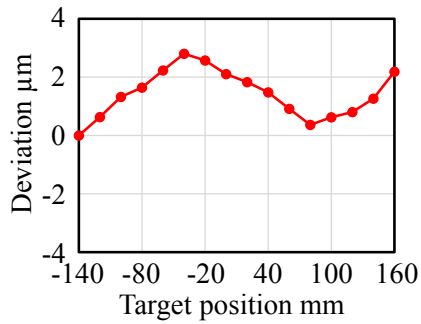


(b) Positioning error of X-axis

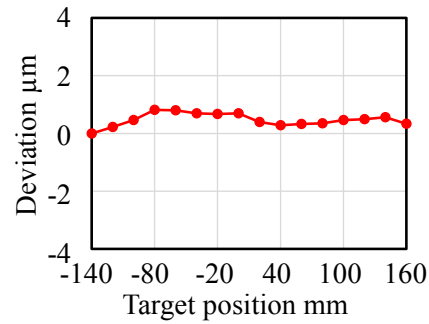
Figure 4 Measurement setup for error motions



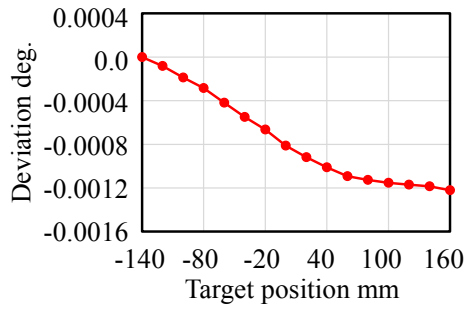
(a) Positioning deviation (E_{xx})



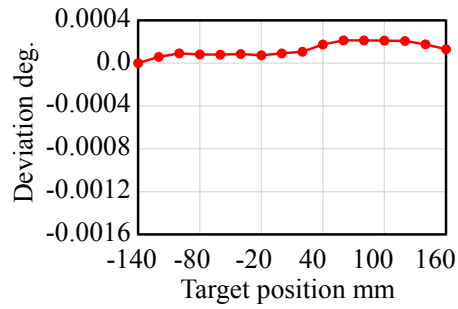
(b) Straightness deviation (E_{yx})



(c) Straightness deviation (E_{zx})



(d) Angular deviation (E_{Bx} , pitch)



(e) Angular deviation (E_{Cx} , yaw)

Figure 5 Measured results of X-axis error motions

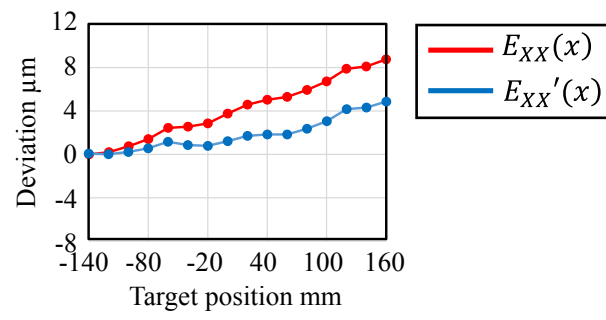
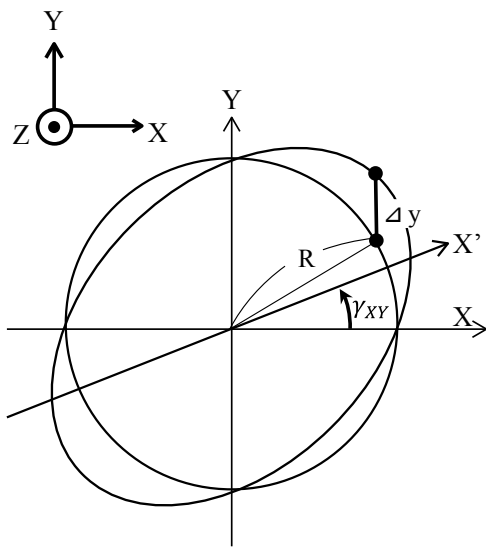
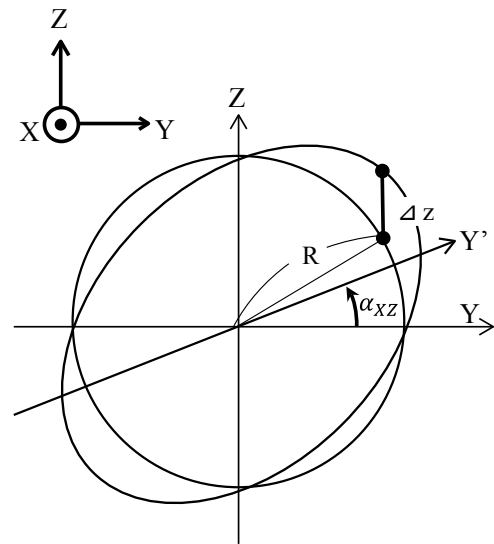


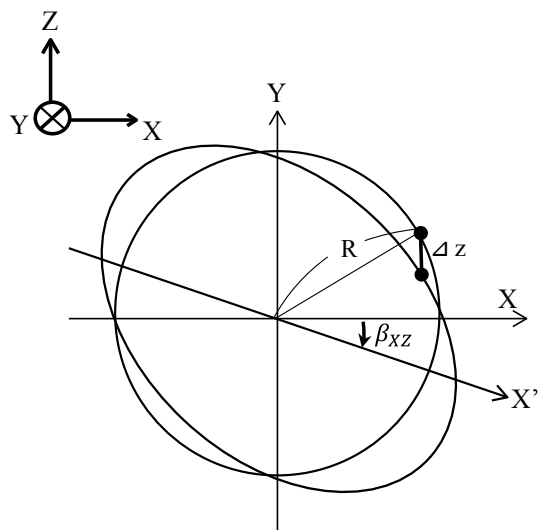
Figure 6 Comparison before and after conversion



(a) XY plane

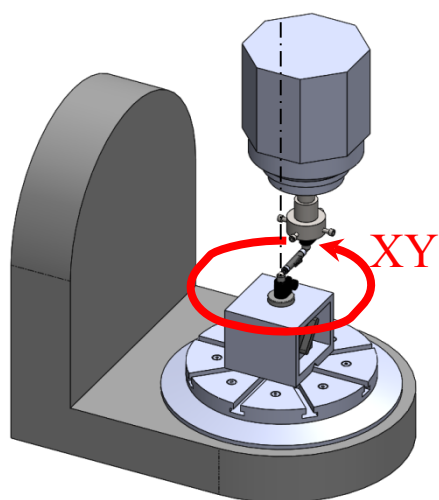


(b) YZ plane

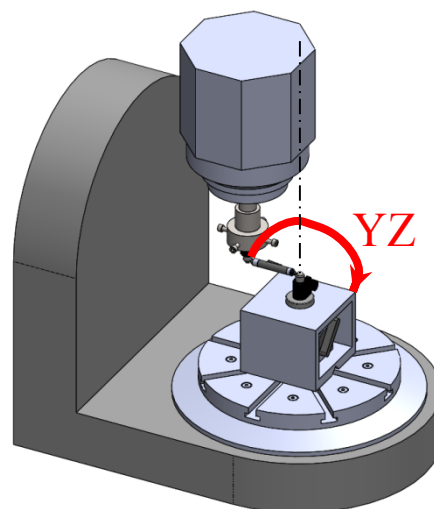


(c) ZX plane

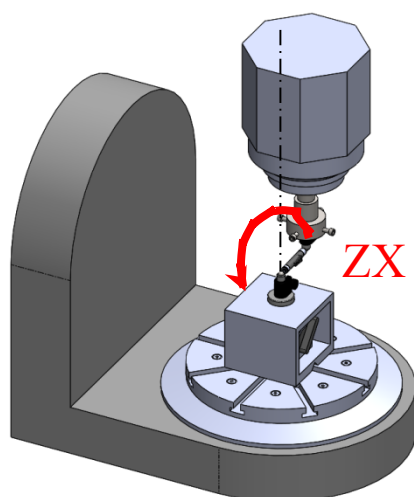
Figure 7 Influence of squareness errors



(a) XY plane



(b) YZ plane



(c) ZX plane

Figure 8 Schematics of three types of circular tests

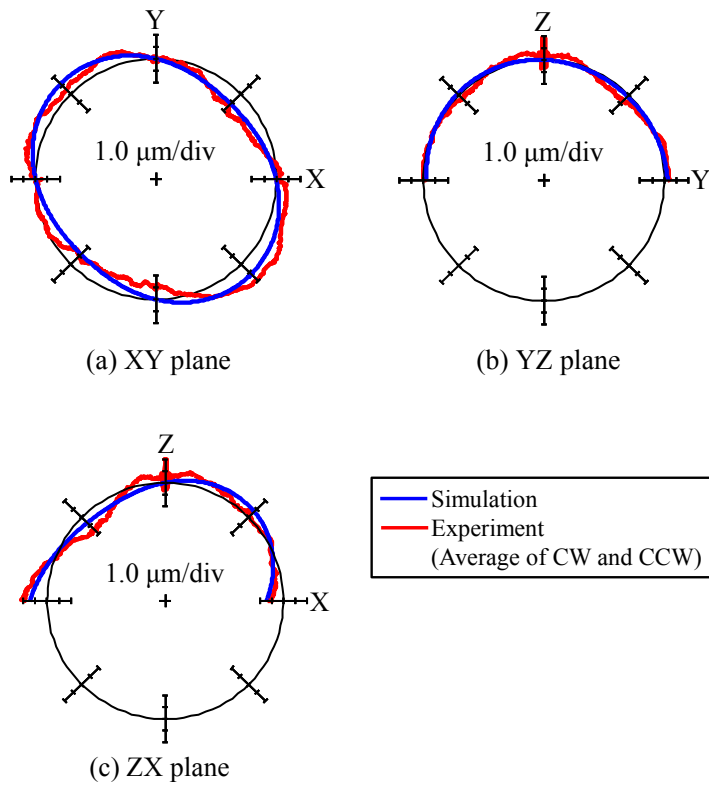


Figure 9 Comparison of measured and simulated circular trajectories

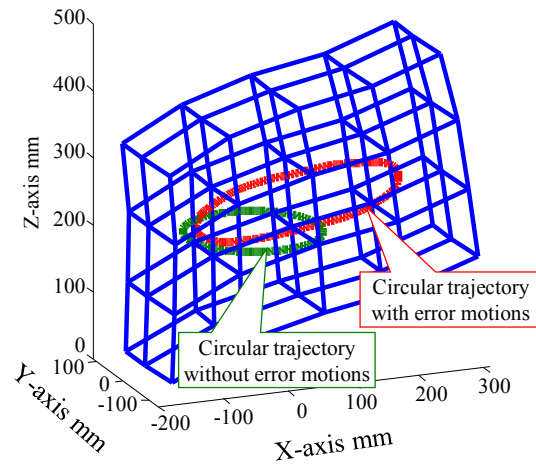


Figure 10 Estimated volumetric error

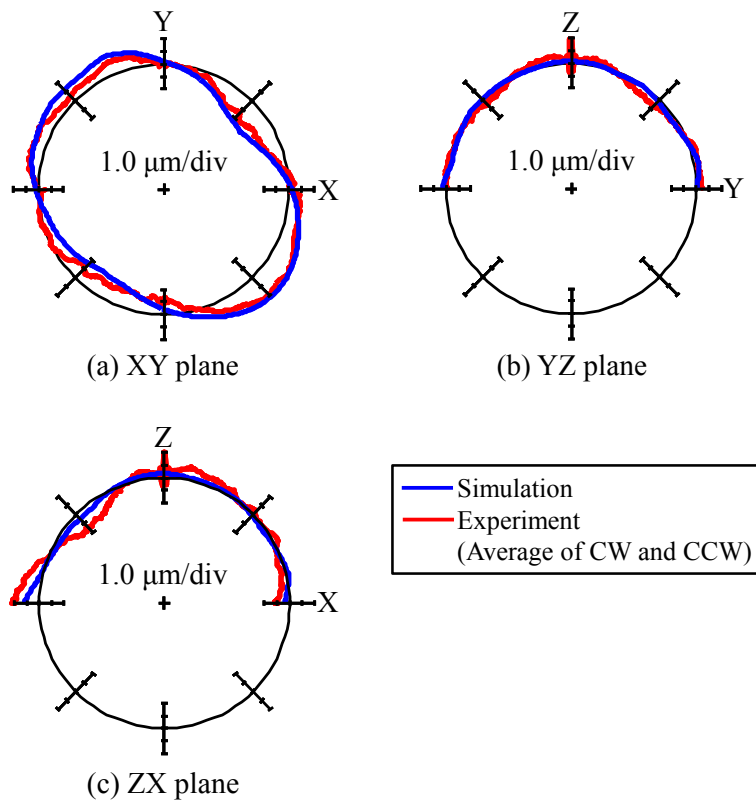


Figure 11 Comparison of measured circular trajectories and simulation trajectories with error motions

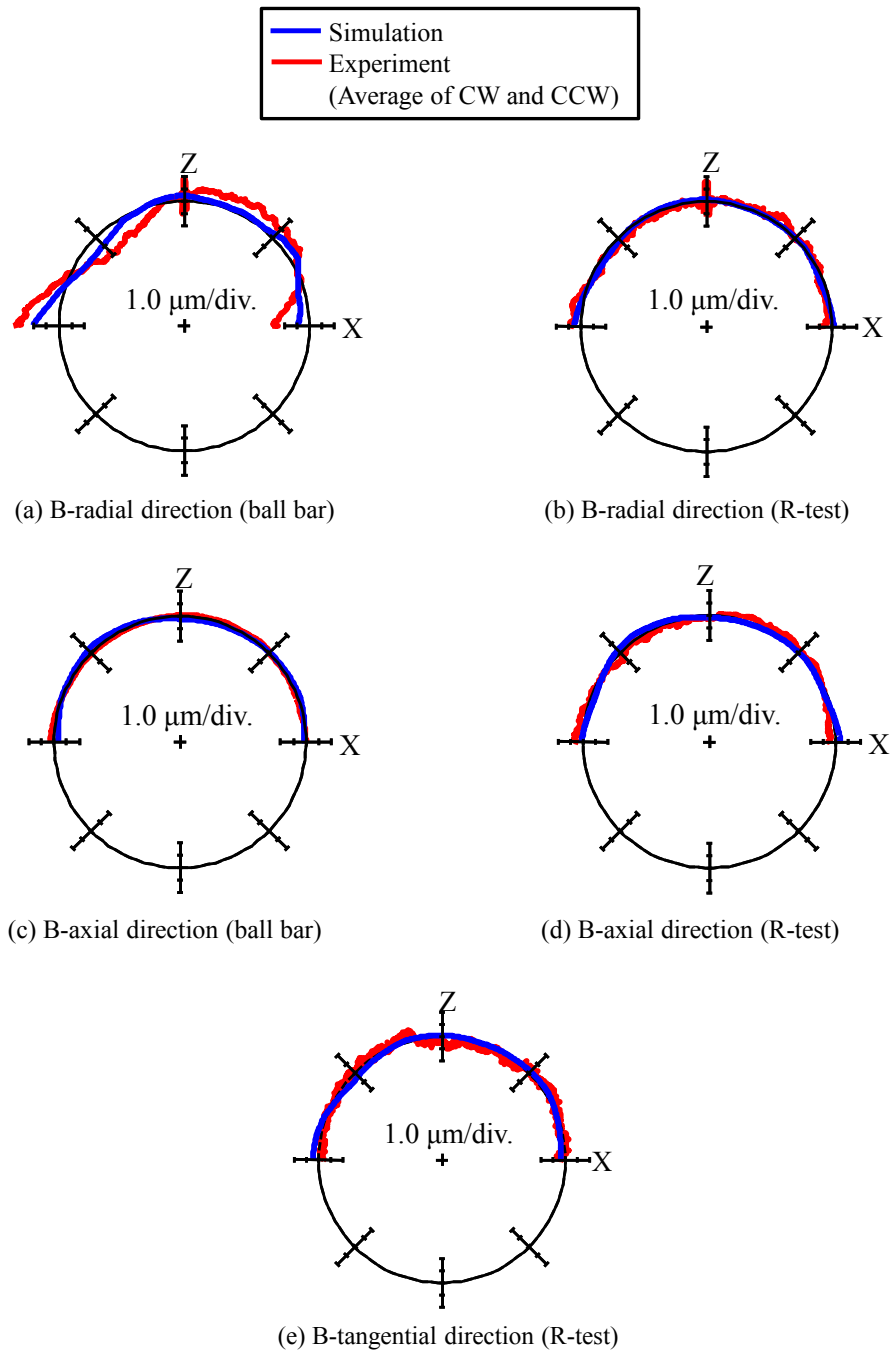


Figure 12 Comparison of influence of error motions of linear axes on simultaneous three-axis motion accuracy (B- and ZX-axes)

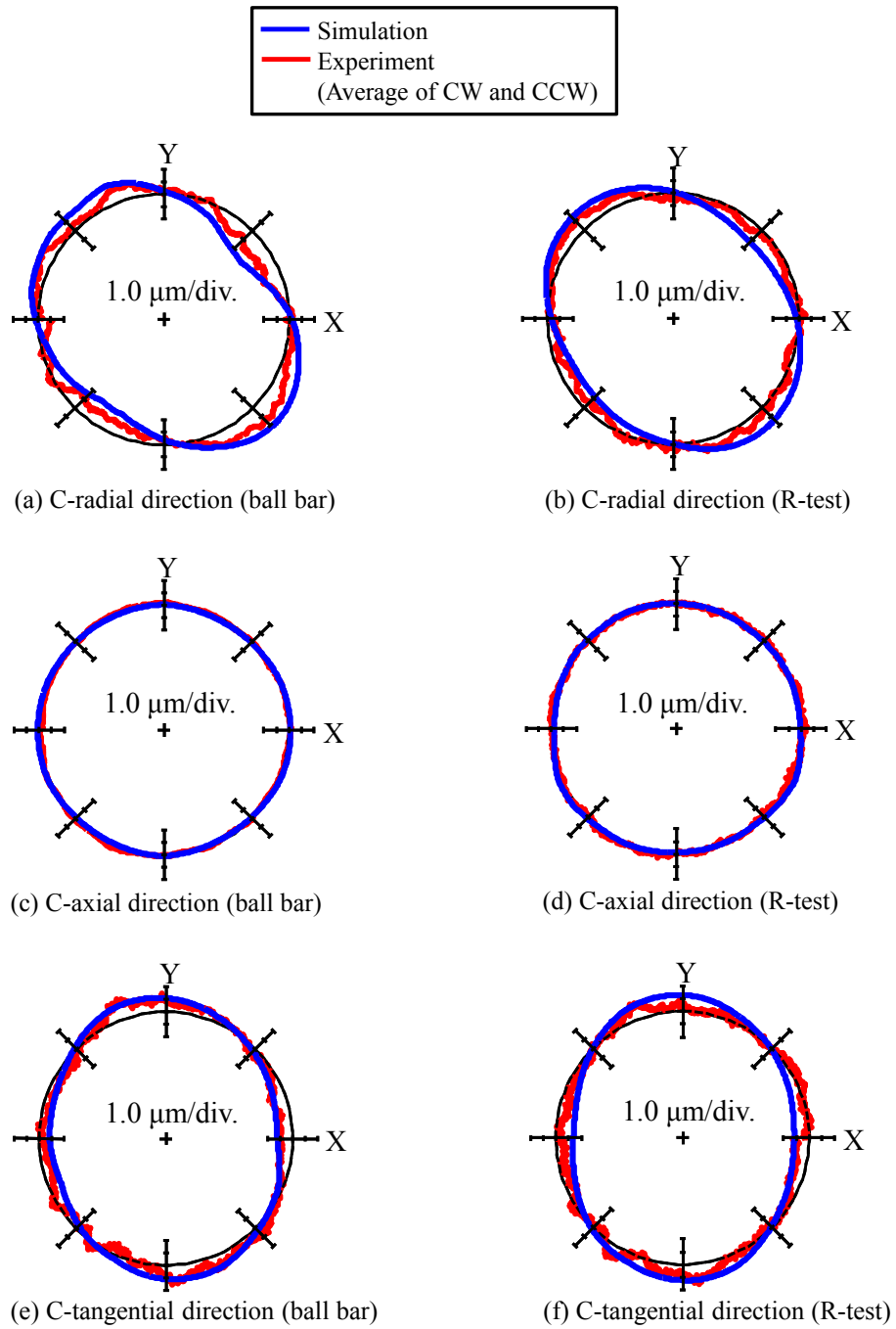


Figure 13 Comparison of influence of error motions of linear axis on simultaneous three-axis motion accuracy (C- and XY-axes)

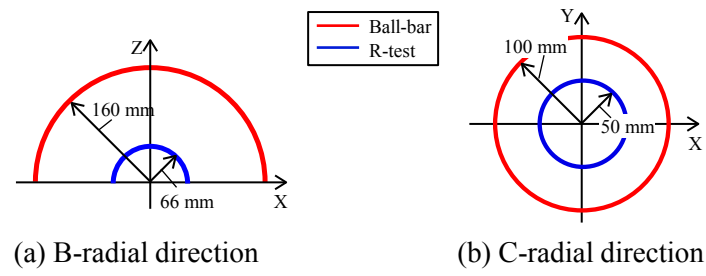
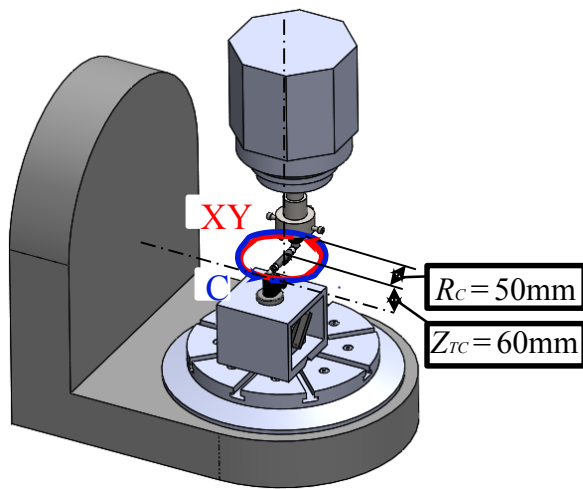
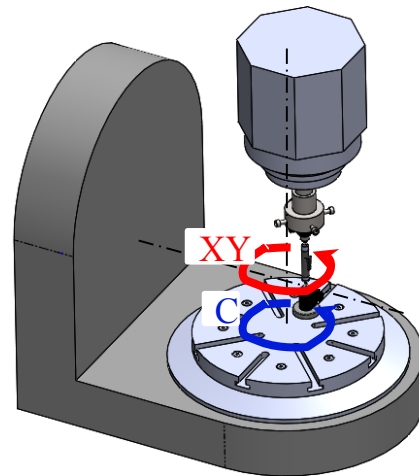


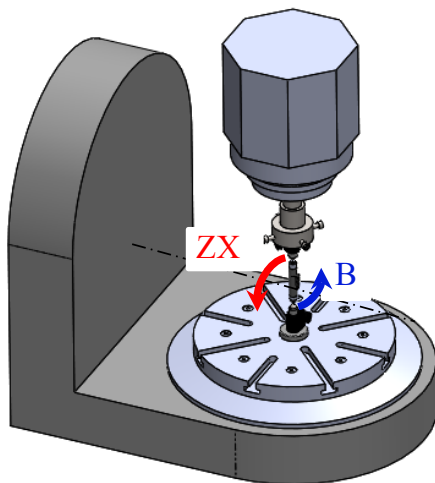
Figure 14 Comparison of trajectory of linear axes for measurements



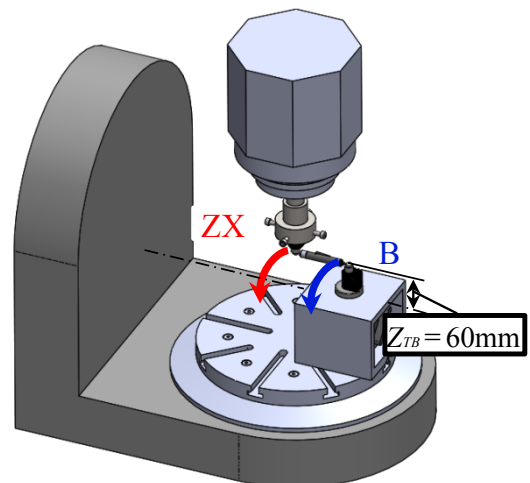
(a) C-radial direction



(b) C-axial direction



(c) B-radial direction



(d) B-axial direction

Figure 15 Simultaneous three-axis motion measurement using ball bar with identical motion trajectory of linear axes with R-test

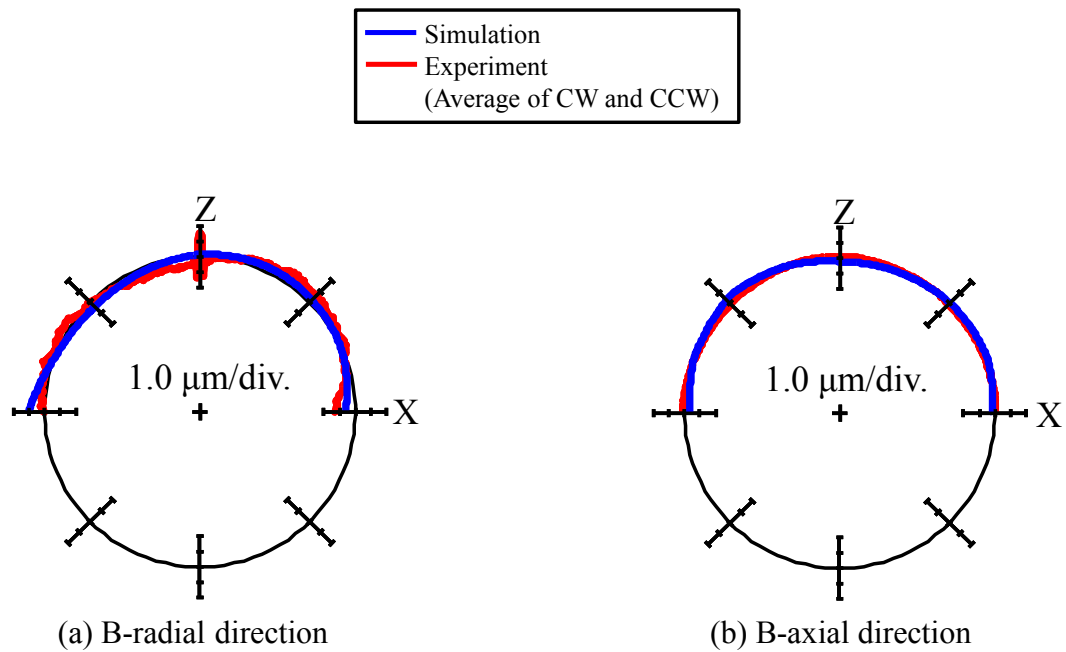


Figure 16 Measured and simulated results of ball bar measurement with identical motion trajectory of linear axes with R-test (B- and ZX-axes)

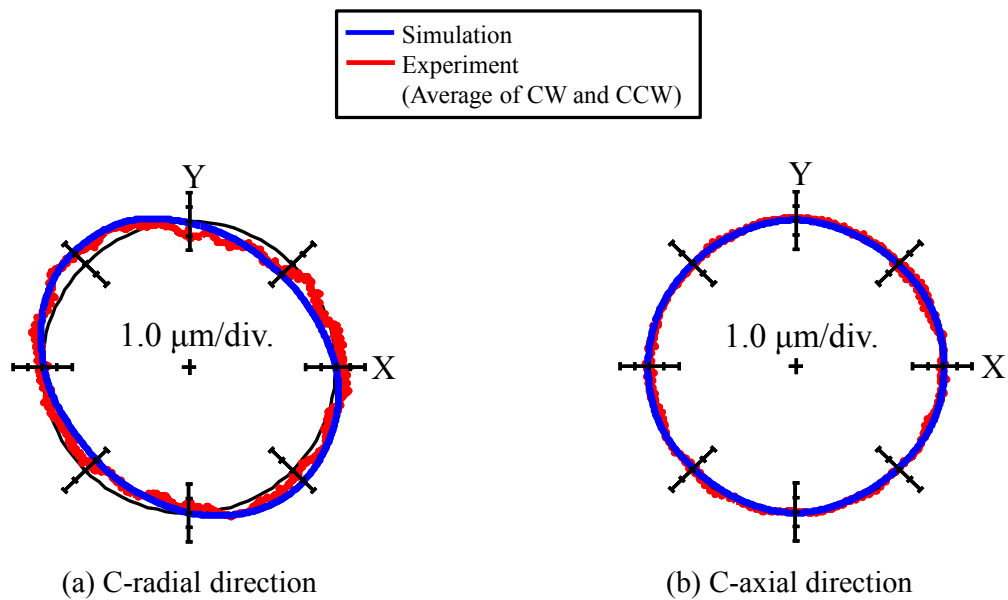


Figure 17 Measured and simulated results of ball bar measurement with identical motion trajectory of linear axes with R-test (C- and XY-axes)